

Article

Optimization of H₂ Production through Minimization of CO₂ Emissions by Mixed Cultures of Purple Phototrophic Bacteria in Aqueous Samples

I.A. Vasiliadou ^{1,2} , J.A. Melero ¹ , R. Molina ¹ , D. Puyol ^{1,*}  and F. Martinez ¹

¹ Department of Chemical and Environmental Technology, ESCET, Rey Juan Carlos University, 28933 Móstoles, Spain; ioavasil@env.duth.gr (I.A.V.); juan.melero@urjc.es (J.A.M.); raul.molina@urjc.es (R.M.); fernando.castillejo@urjc.es (F.M.)

² Department of Environmental Engineering, Democritus University of Thrace, 67100 Xanthi, Greece

* Correspondence: daniel.puyol@urjc.es; Tel.: +34-91-488-80-95

Received: 15 June 2020; Accepted: 13 July 2020; Published: 15 July 2020



Abstract: One of the current challenges in the treatment of wastewater is the recovery and/or transformation of their resources into high value-added products, such as biohydrogen. The aim of the present study was to optimize the production of hydrogen by mixed cultures of purple phototrophic bacteria (PPB), targeting in low CO₂ emission. Batch assays were conducted using different carbon (malic, butyric, acetic acid) and nitrogen (NH₄Cl, Na-glutamate, N₂ gas) sources by varying the chemical oxygen demand to nitrogen ratio (COD:N 100:3 to 100:44), under infrared radiation as sole energy source. Malate-glutamate (COD:N 100:5.5) and malate-NH₄-N (COD:N 100:3) fed cultures, exhibited high H₂ production rates of 2.3 and 2.5 mLH₂/Lh, respectively. It was observed that the use of glutamate decreased the CO₂ emission by 74% (13.4 mLCO₂/L) as compared to NH₄-N. The H₂ production efficiency achieved by organic carbon substrates in combination with glutamate, was in the order of malic (370 mLH₂/L) > butyric (145 mLH₂/L) > acetic acid (95 mLH₂/L). These substrates entailed partitioning of reducing power into biomass at 64%, 50% and 48%, respectively, whereas reductants were derived to biohydrogen at 5.8%, 6.1% and 2.1%, respectively. These results suggest that nitrogen source and carbon dioxide emissions play an important role in the optimization of hydrogen production by PPB.

Keywords: wastewater; biohydrogen; carbon dioxide; malic acid; Na-glutamate

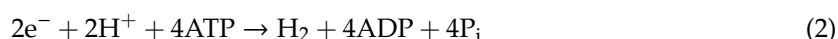
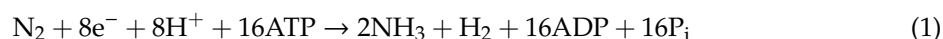
1. Introduction

Nowadays, human activities associated with food production, agriculture, domestic and industry generate considerable amounts of waste effluents rich in nutrients and organic compounds. Uncontrolled disposal of these wastes alters severely the biogeochemical cycles of the global ecosystems and can cause great damage to the environment. Public or private associations responsible for water sanitation invest lot of energy in wastewater treatment plants just for the destruction of organic matter and removal of nutrients, in order to avoid the contamination of water bodies. However, wastewater treatment processes can be upgraded into sustainable biorefineries for release and recover energy and nutrients within the concept of circular economy and the water-energy-food nexus [1,2].

The use of photosynthetic organisms for partitioning of resources from wastewater has received considerable attention worldwide, since is an environmental-friendly and a low energy alternative, compared to physical separation processes, such as membrane technologies [1,3]. Microalgae have been widely used for nutrients' partitioning from the liquid into their solid phase from wastewater, however, they form macroscopic structures that hinders their settleability, which makes hard their

harvesting [4]. This is, in fact, one of the major limitations for cost-effective wastewater treatment [5]. Alternatively, purple phototrophic bacteria (PPB) are able to simultaneous partition of organics, nitrogen and phosphorous and therefore have been proposed as a new partitioning approach for wastewater treatment [1,6]. PPB are fast growing organisms that can be easily isolated from sources such as soil, freshwater, marine, and sewage [7]. They grow via anoxygenic photosynthesis by converting low energy infrared light into chemical energy, in the form of adenosine triphosphate (ATP) [8]. PPB have an extremely versatile metabolic system, but the most interesting metabolic pathway involves photoheterotrophic growth using sugars or organic acids as electron donors and carbon source in presence of light, which also entails CO₂ fixation or emissions depending on the overall redox state of the system [9,10].

PPB can harvest and accumulate electrons during the cyclic anoxygenic photosynthesis, in the form of reduced cofactors. Excess of reductants is handled through CO₂ fixation via the Calvin cycle or by H₂ release [11]. Hydrogen production is an ATP-driven process occurred under nitrogen-fixing conditions or by directly dissipating electrons via ferredoxin oxidation in the nitrogenase/hydrogenase enzyme complex at the end of the electron transport chain [12,13]. The theoretical stoichiometries for hydrogen production in the presence and absence of dinitrogen gas are presented in Equations (1) and (2), respectively [14].



Highly reduced carbon sources relative to PPB biomass (e.g., butyrate), are expected to promote hydrogen production as compared to more-oxidized substrates (e.g., acetate and malate) [10]. However, it has been previously reported for both mixed and pure cultures of PPB, that H₂ yields are not strictly co-related with the carbon oxidation state [15–17]. Other factors affecting the H₂ yield from different organic substrates is the amount of organic carbon stored as polymers such as polyhydroxybutyrate (PHB), as well as the Calvin cycle flux competing for electrons [16]. Moreover, an important factor non correlated with carbon substrates, is the nitrogen source, since the presence of NH₄-N represses nitrogenase synthesis of PPB and therefore H₂ production [14].

Ammonium salts, reversibly inhibit the enzyme, which is able to recover its activity after the consumption of ammonium. It has been, also reported that inhibition may occur, by the formation of ammonium during the consumption of non-ammonium nitrogen sources, such as glutamate. Nevertheless, glutamate is considered an excellent substrate for hydrogen production, since it serves simultaneously as carbon and nitrogen source [18]. Finally, dinitrogen, which serves as the natural substrate of nitrogenase, inhibits the hydrogen production rate, since N₂ fixation and biohydrogen production are two competing processes [19].

Biological hydrogen production generates a renewable environmental-friendly biofuel, that produces H₂O upon combustion [20]. Oxygenic (algae, cyanobacteria) and anoxygenic (PPB) photosynthetic hydrogen production, also known as photo-fermentation, is considered the absolute renewable source, since it requires a supply of light energy and H₂O or organic electrons donors [21], respectively. However, H₂ production from the photo-fermentation of organic compounds may lead to the simultaneous production of CO₂ [22], a key greenhouse gas that drives global climate change.

PPB have been widely assessed for industrial wastewater treatment or transformation of organic streams coming from biorefineries towards organics recovery and/or H₂ production [9,17,20,23–34]. However, most of these studies use pure cultures [9,17,22,25,26,29,30,35,36] and do not deal with the factors involved in CO₂ emissions. Controlling the driving factors for CO₂ releasing, is key for reducing greenhouse gas emissions in photo-fermentation processes.

This study aims to evaluate the performance of mixed PPB cultures for biohydrogen production from wastewater, while minimizing CO₂ emissions. Optimization basis relies on the use of different organic carbon sources and organic and inorganic nitrogen substrates, applying a wide range of COD

to nitrogen ratio (100:3 to 100:44) to evaluate the production yield and the CO₂ production. An electron balance method based on chemical oxygen demand (COD) was used to determine the partitioning of electrons into H₂ and PPB growth.

2. Materials and Methods

2.1. Chemical Compounds

The chemical compounds that were used in this study were purchased from Sigma-Aldrich. Stock solutions (20 gCOD/L) of L-malic acid (C₄H₆O₅), butyric acid (C₄H₈O₂), propionic acid (C₃H₆O₂), acetic acid (C₂H₄O₂) and ethanol (C₂H₆O) were prepared separately in ultra-pure water and stored at 4 °C. Stock solutions (5 gN/L) of ammonium chloride (NH₄Cl) and L-glutamic acid monosodium salt monohydrate (Na-glutamate, C₅H₈NNaO₄·H₂O) were prepared separately in ultra-pure water and stored at 4 °C. Finally, nitrogen gas (N₂) was used as external gaseous nitrogen source. The pH in stock solutions was adjusted to 7.

2.2. Enrichment of Purple Phototrophic Bacteria (PPB)

The mixed culture of purple phototrophic bacteria (PPB) was enriched from wastewater taken from a pilot-scale WWTP at Rey Juan Carlos University (Mostoles, Madrid, Spain). Enrichment process was performed following the procedure outlined by Vasiliadou et al. [15]. Briefly, a 1 L suspended growth photo-bioreactor (PhBR) containing synthetic wastewater (SW) as growth medium was inoculated with 20% *v/v* of domestic wastewater. The SW was prepared with tap water containing 5 organic carbon sources (acetic acid, malic acid, propionic acid, butyric acid and ethanol) (total COD 1.2–1.6 gCOD/L), NH₄Cl (0.06–0.13 gN/L) as well as 1 mL/L micro-nutrient and 100 mL/L of macro-nutrient solution, which were prepared according to Ormerod et al. [37]. Subsequently, the SW in the reactor was flushed with argon gas to remove dissolved oxygen in order to achieve anaerobic conditions.

The incubation was performed by illuminating the PhBR with LED lamps (850 nm) to provide near infra-red (NIR) light source (Figure 1). The surface of the PhBR was covered with UV-VIS absorbing foil (ND 1.2 299, Transformation Tubes, Banstead, UK), in order to absorb ca. 90% of the wavelength <750 nm. The average light intensity on the outside PhBR surface was 10 W/m², which results in 512 W/m³ at a surface to volume (V_L) ratio of 51.2 m²/m³. These conditions can be considered as non-limiting in irradiation needs [38]. Figure 2, presents a contour diagram, that was constructed using Matlab software, illustrating the IR light intensity measured on different heights around the surface of the PhBR. The measurements covered a surface area of 512 cm² (P×H = 32 × 16 cm) (Figure 1). The whole acclimation period (around 40 days), PPB culture was kept at room temperature (25 ± 1 °C), while the pH was weekly adjusted to 6.8 ± 0.1. The PhBR was operated using 99% SW replacement with fresh medium on a weekly basis. The system was operated for six weeks. The total COD added in the PhBR during the 6 weeks of operation was in the range of 1.2–1.6 gCOD/L, with ammonium nitrogen concentration of ca. 0.06–0.13 gN/L. The enrichment of PPB was determined by detecting the presence of Bacteriochlorophylls (*BChl*) and carotenoids in liquor samples of the PhBR using VIS-IR spectra analyses.

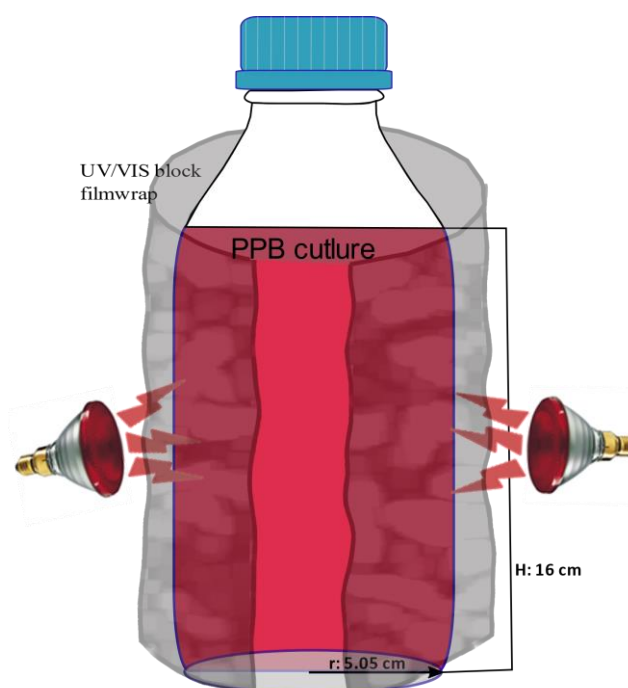


Figure 1. Photo-bioreactor's set-up.

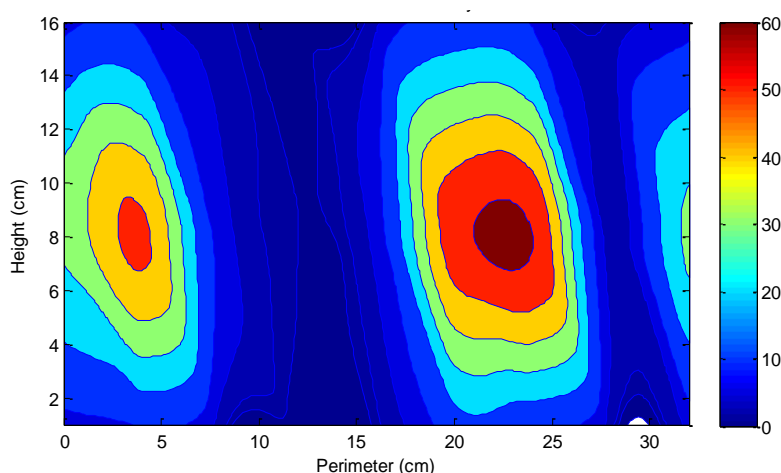


Figure 2. Infrared (IR) light intensity (W/m^2) on the PhBR surface.

2.3. Batch Assays of PPB

Batch experiments were conducted using serum bottles (160 mL) with a working volume of 100 mL, containing 99 mL of SW medium (as previously described) and 1% *v/v* inoculum of PPB enriched culture, that was grown in the PhBR. In the SW, different organic carbon and nitrogen sources were examined. All experiments were performed using ca. 2 gCOD/L of carbon source (malic-, butyric- and acetic- acid). On the other hand, nitrogen source concentrations were varying from 75 to 600 mgN/L (NH_4Cl as inorganic N source and Na-glutamate as organic N source) or the corresponding to the liquid-gas equilibrium with dinitrogen gas filling the headspace of the serum bottles (60 mL of N_2). Control experiments without PPB enriched culture were conducted under sterilized conditions for all the conditions tested in this study. The conditions under which each batch assay was performed are given in Table 1. As shown in Table 1, the carbon and nitrogen substrates were tested in different combinations, using a wide range of COD:N ratios (100:3.8–100:30), considering only the COD of organic substrate and the N of the nitrogen substrate. It should be noted that these COD:N ratios were initially calculated based on the theoretical concentrations of organic and nitrogen substrates

added. Therefore, Table 1 presents also the actual COD:N for each experiment (R1–R14), as resulted from the experimental measurements, considering also the amount of COD came from the use of Na-glutamate. It should be noted, that during experiment R14, the nitrogen concentration per liquid volume added as N₂ was 650 mgN/L. The N₂ from the gas phase was gradually diluted into the liquid phase, while based on Henry's Law the maximum concentration of dissolved N₂ each time could not exceeded the 17 mgN/L.

Table 1. Experimental condition of batch assays of purple phototrophic bacteria (PPB) using different carbon and nitrogen sources.

RUN Number	Carbon Source	Nitrogen Source	Nitrogen (mgN/L)	COD-Substrate to N Ratio ^a COD:N	Measured COD to N Ratio ^b COD:N
R1	Malic acid	NH ₄ Cl	75	100:3.8	100:3
R2			150	100:7.5	100:6.8
R3			300	100:15	100:12.1
R4			600	100:30	100:33.8
R5	Acetic acid	NH ₄ Cl	75	100:3.8	100:2.9
R6			150	100:7.5	100:8.6
R7			300	100:15	100:15.6
R8			600	100:30	100:44
R9	Malic acid	Na-glutamate	75	100:3.8	100:2.3
R10			150	100:7.5	100:4.6
R11			300	100:15	100:5.5
R12	Butyric acid	Na-glutamate	300	100:15	100:6.9
R13	Acetic acid	Na-glutamate	300	100:15	100:6.7
R14	Malic acid	N ₂ gas	650 ^c	100:33	100:36

^a COD-substrate to N ratio, considering only the COD of organic substrate and the N of the nitrogen substrate;

^b Measured COD to N ratio, considering also the COD content of glutamate; ^c Nitrogen concentration per liquid volume added as N₂.

The pH at the beginning of each experiment was adjusted to 6.8 ± 0.1 . After the preparation of the bottles, their liquid mediums were flushed with argon for 10 min and closed with rubber stoppers with aluminum seals. Subsequently, the headspace of the bottles was flushed with argon for 2 min. The bottles where nitrogen gas was used, were flushed with N₂ gas. The bottles were shaken at 120 rpm and 25 ± 1 °C (Orbital shaker, optic ivymen system) and illuminated using LED lamps from the left and right-top of the shaker, providing an average uniform IR intensity of 20 W/m². The duration of each experimental run was 7 days.

Chemical oxygen demand (COD), total Kjeldahl Nitrogen (TKN), ammonium nitrogen and PPB and organic acids' concentrations, were determined at the beginning and at the end of each experimental run. Moreover, throughout each experiment 2 mL of liquid samples (which were replaced with sterile degassed water) were taken from the liquid phase at different time intervals, to evaluate organic acids' assimilation and PPB growth. Gas samples were taken from the serum bottles and were analyzed periodically to evaluate hydrogen production and CO₂ evolution. Biological and control experiments were conducted in duplicate. Runs R4–R8 were conducted initial once, in order to check the potential of H₂ production under these conditions. The experiments were not repeated twice for time-saving reasons, since the first screening showed no encouraging results.

2.4. Analytical Methods

All liquid samples were analyzed after filtering with a 0.45 µm nylon filter (Chrodisc filter/syringe, CHMLab, Barcelona, Spain). Total chemical oxygen demand (COD), total Kjeldahl Nitrogen (TKN),

biomass absorbance at 660 nm (optical density) and VIS/NIR spectra were determined using unfiltered samples. Total and soluble COD were determined using a dichromate-reflux colorimetric method [39]. The TKN of filtered and unfiltered samples were determined by the standard Kjeldahl procedure (Gerhardt TNK, Vapodest 450, Königswinter, Germany). The $\text{NH}_4\text{-N}$ was analyzed using Spectroquant Ammonium Test (Merck, Darmstadt, Germany). The VSS concentration (gVSS/L) was measured according to standard methods [39]. The optical density of PPB biomass at 660 nm was measured using UV-VIS spectrophotometer (V-630, Jasco, Madrid, Spain). The concentration of PPB was calibrated using a standard curve of optical density against volatile suspended solids (gVSS/L). The detection of *BChl* and carotenoids of PPB was performed by VIS-NIR spectra (400–950 nm) (V-630, Jasco, Madrid, Spain). The pH was measured using a pH meter (Crison GLP22, Hach Lange, Loveland, CO, USA). Illuminance was measured with a VIS-NIR spectroradiometer (STN-Bluewave-V, MTB, Madrid, Spain). The concentrations of volatile fatty acids (VFAs, malic, acetic and butyric acids) were analyzed using high performance liquid chromatography (HPLC) (Varian 356-LC, Agilent Technologies, Santa Clara, CA, USA), using refractive index (RI) detector and MetaCarb 67H 300 × 6.5 mm column (Agilent Technologies, Santa Clara, CA, USA). The volume of the gas accumulated in the headspace of the bottles was determined using a Boyle-Mariotte Apparatus (3B Scientific S.L., Hamburg, Germany). The gas composition was analyzed using a 7820A GC system equipped with a 3Ft 1/8 2 mm Poropak Q 80/100 SS column, a 6Ft 1/8 2 mm Poropak Q 80/100 SS column and a 6Ft 1/8 2 mm MolSieve 5A 60/80 SS column, a fitting external Luer lock and a thermal conductivity detector (TCD) (Agilent Technologies, Santa Clara, CA, USA).

2.5. Statistical Analysis

Experimental data of experiments were used to calculate average values (Equation (3)) and standard deviations (Equation (4)).

$$\bar{Y} = \frac{\sum_{i=1}^n Y_i}{n} \quad (3)$$

$$SD = \sqrt{\frac{\sum_{i=1}^n (Y_i - \bar{Y})^2}{n - 1}} \quad (4)$$

where \bar{Y} is the average of the measured values, SD is the standard deviation, Y_i are the experimental values and n is the total number of data.

Confidence Interval on the mean was computed as follows (Equation (5)):

$$CI = \bar{Y} \pm Z_{95} \cdot \frac{SD}{\sqrt{n}} \quad (5)$$

where Z_{95} is the number of standard deviations extending from the mean of a normal distribution required to contain 0.95 of the area. With a normal distribution, 95% of the distribution is within 1.96 standard deviations of the mean.

3. Results and Discussion

3.1. PPB Culture Enrichment

Figure 3a presents the biomass growth, the soluble COD degradation and the initial ammonium concentration during a 6-weeks enrichment period of the mixed PPB culture. Each operating cycle of the PhBR lasted 7 days (see Section 2.2). After a 2-weeks period, a stable behavior of the system during the next 4 cycles in terms of biomass production rate (0.12 ± 0.01 gVSS/Ld) and biomass yield (0.64 ± 0.08 gVSS/gCOD) in each cycle, was observed. COD consumption rate throughout this steady state was 0.18 ± 0.02 gCOD/Ld. PPB biomass enrichment was evidenced through the accumulation of *BChl* and carotenoids in the mixed culture. Figure 3b shows the absorption spectra that represent PPB growth at different time intervals, i.e., at the end of 2nd, 3rd and 5th cycle. The peaks with maximum

absorbance at 590, 805, and 865 nm represents the absorption maxima for *BChla*. It was observed that during the 2nd cycle PPB enrichment was sufficient with a high proportion of *BChla* as evidenced by the sharp increase of the $Abs_{805,865}/Abs_{660}$ ratio as compared to the 1st cycle (1.0 to 1.6) [40]. It is well known, that PPB under anaerobic conditions and NIR irradiation express their photosynthetic system via bacteriochlorophyll [41] which associated with carotenoid pigments to a light-harvesting complex [8]. The absorption spectrum of carotenoids appeared in the spectral range between 400 and 550 nm [42]. PPB produce a subclass of the molecules commonly referred to as open-chain carotenoids pigments that protect the cells from photooxidative damage [10].

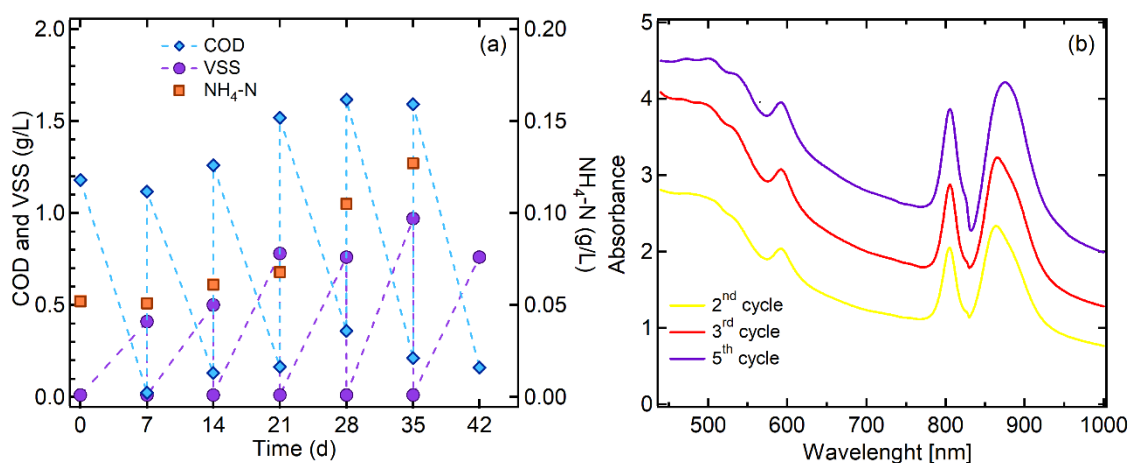


Figure 3. (a) COD assimilation, biomass growth and NH_4-N concentration added throughout the weekly operation photo-bioreactor and (b) Absorbance spectra (440–1000 nm) of PPB in culture medium for three cycles.

Regarding community composition, it has been previously stated that an Abs_{805}/Abs_{660} ratio higher than 1.0 indicates a very high dominance of PPB in the bacterial community, with PPB presence (based on Illumina MiSeq analysis on the 16S RNA gene) higher than 50% [40]. In addition, *BChla* is indicative of species from genera like *Rhodobacter* sp., *Rhodospseudomonas* sp. and *Rhodospirillum* sp., which were found as dominants in domestic wastewater enrichments cultivated under anaerobic photo-heterotrophic environments [3,6]. These genera commonly have a very high efficiency of carbon usage, with biomass yield values close to 1.0 (COD basis), which are very similar to the values reported in this study. These evidences lead to the assumption, that the enriched culture of the present study, was strongly dominated by PPB.

3.2. Effect of Nitrogen Sources on H_2 and CO_2 Production

In this study, the effect of nitrogen source on the H_2 production process by a mixed PPB culture, was investigated using malic, as organic carbon source and ammonium chloride, Na-glutamate and N_2 gas, as nitrogen sources. Table 2 summarizes the cell growth rate, the substrate degradation rate, the H_2 production rate, the H_2 yield and the CO_2 production. Figure 4 shows the time profiles using malic acid and NH_4Cl as carbon and nitrogen sources, respectively. Figure 4a,c and d represents the malic acid degradation and PPB growth using 75, 150 and 300 $mgNH_4-N/L$ (runs R1 – R3) and ca. 1.1 gC/L (ca. 2.2 $gCOD/L$) of two experimental trials (1 and 2), while Figure 4b shows the H_2 and CO_2 production by PPB using 75 $mgNH_4-N/L$ (run R1). As shown in Table 2, higher H_2 production (381.6 mLH_2/L) was achieved at the NH_4-N concentration of 75 $mgNH_4-N/L$ (5.4 mM ammonium, R1), compared to the concentrations of 150–600 $mgNH_4-N/L$ (10.7–42.9 mM ammonium, R2 – R4), where little or no H_2 generation was detected. It has been previously reported that ammonium concentrations higher than 20 μM strongly inhibit the activity of nitrogenase in axenic cultures of *R. sphaeroides* [10]. In addition, Kim et al. [43] reported that H_2 production by *R. sphaeroides* was inhibited at ammonium concentrations higher than 2 mM. The results obtained suggest that the mixed

PPB culture used in this study, had tolerance to the ammonium concentrations as high as 5 mM. Interestingly, Tichi and Tabita [44] reported that some PPB species, such as *Rhodobacter capsulatus*, in the absence of a functional Calvin cycle or any other exogenous electron acceptor, are able to develop alternative electron acceptor pathways to preserve their intracellular redox state. In the presence of high ammonium levels, *R. capsulatus* can derepress the synthesis of the dinitrogenase enzyme complex, allowing the dissipation of excess reducing equivalents towards H_2 production.

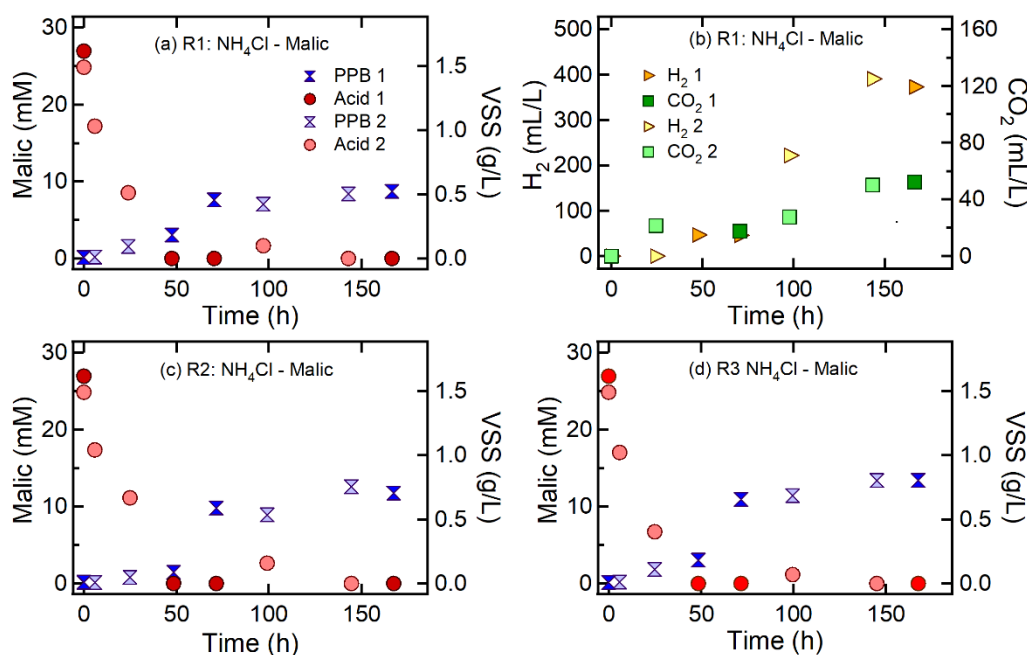


Figure 4. (a) Malic acid uptake and PPB growth for R1, (b) gases production for R1, (c) malic acid uptake and PPB growth for R2 and (d) malic acid uptake and PPB growth for R3.

It should be noted, that during H_2 production using $75 \text{ mg}NH_4\text{-N/L}$ (5.4 mM ammonium, R1), significant CO_2 production was observed ($51.2 \text{ mL}CO_2\text{/L}$, Figure 4b, Table 2). The oxidation of malic acid, which is more oxidized than PPB biomass, results in CO_2 production via TCA cycle [11]. A mass balance over liquid and gas phases on CO_2 concentration, using Henry's law and experimental pH values, provided that the produced CO_2 was similar to the theoretically expected production based on the stoichiometry of malic acid, with a ratio of $H_2:CO_2$ of 1:1 compared to the theoretical ratio of 3:2.

Subsequently, experiments were conducted using malic acid as carbon source (ca. 26 mM or 1.2 gC/L, and ca. 2.4 gCOD/L) and Na-glutamate as nitrogen source. The nitrogen concentrations used were 75–300 mgN/L. In the cases of runs R9–R11, COD:N ratios were significantly different from the COD-substrate to N ratios, due to the carbon content of Na-glutamate (Table 2). Figure 5 shows the time profiles using Na-glutamate and malic acid as nitrogen and carbon source, respectively. Figure 5a–c illustrates the malic acid degradation and PPB growth using 75, 150 and 300 mgN/L (runs R9–R11) of two experimental trials (1 and 2), while Figure 5d shows the H_2 and CO_2 production by PPB using 300 mgN/L (run R11). Increasing initial glutamate concentrations caused a rise in the H_2 production values (Figure 6, Table 2). The highest H_2 production in these experiments was observed for a concentration of 300 mgN/L of glutamate (R11: $370 \text{ mL}H_2\text{/L}$) (Figure 6, Table 2). It should be noted, that no ammonium accumulation was observed during the experimental runs with Na-glutamate. This is in contrast with other research studies conducted with *R. sphaeroides* strain, reporting that H_2 evolution was significantly suppressed by ammonium ions, which were accumulated proportionally to the concentration of glutamate added [43].

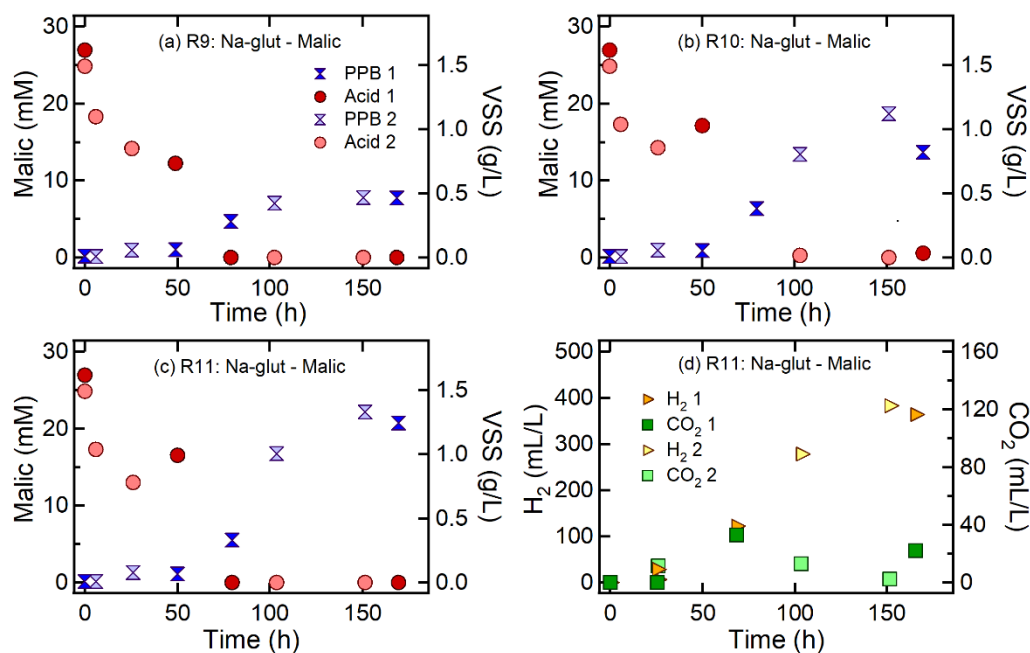


Figure 5. Malic acid assimilation, PPB growth in media supplemented with malic acid and Na-glutamate for (a) R9, (b) R10 and (c) R11 and (d) gases production for R11.

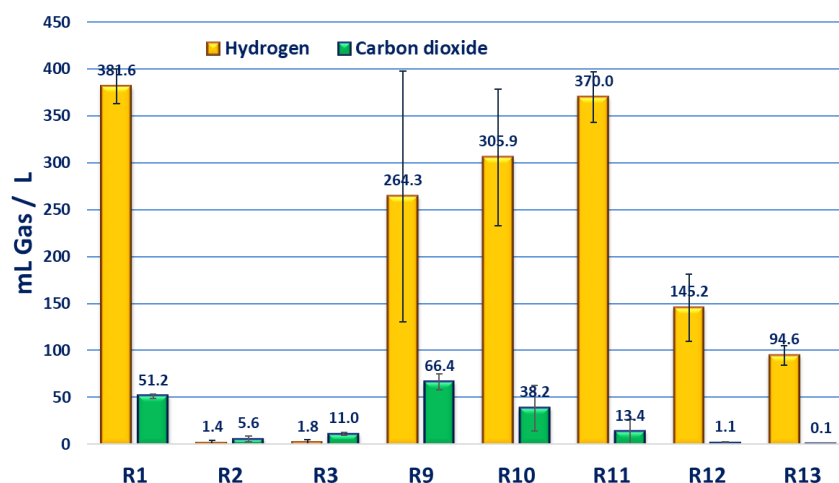


Figure 6. H₂ and CO₂ production under different conditions tested. Error bars present the corresponding CI (95%) for each combination of sources tested.

The H₂ production rate and yield obtained for 300 mgN/L of Na-glutamate (R11), were comparable to those achieved by 75 mgNH₄-N/L (R1) (Table 2). However, the CO₂ gas emission in run R11 was decreased by 74% as compared to run R1b, resulting to the production of 13.4 mLCO₂/L. In addition, results showed an inverse relationship between glutamate addition and CO₂ gas production (Figure 6). The H₂:CO₂ ratios achieved were 1.2:1.5, 1.1:1.7 and 1:0.8 for 75, 150 and 300 mgN/L (R9 – R11), respectively. Interestingly, the CO₂ gas production using Na-glutamate, was negatively correlated with the PPB growth rate achieved during R9–R11, as resulted from linear regression ($y = -15.4x + 118.0$, $R^2 = 0.9122$) of PPB growth rate vs CO₂ (mLCO₂/L). This confirms that CO₂ fixation process is crucial for photoheterotrophic growth [45]. Actually, Wang et al. [45] showed that in the absence of ribulose-1,5-bisphosphate carboxylase/oxygenase, which is the responsible enzyme for CO₂ fixation, the mutant *R. sphaeroides* was not able to grow neither photoautotrophically nor photoheterotrophically using malate as the carbon substrate. PPB growth on oxidized organic substrates, such as malic acid, produces CO₂ due to the substrates' oxidation, which then is re-fixed into cell material using the

Calvin cycle [11]. The electrons needed for this come from the transformation of glutamate during its metabolism, as has been previously reported [15]. Thereby, it can be concluded that an organic N source (N-glutamate) considerably decreases the CO₂ emissions as compared to an inorganic source (ammonium) in photo-fermentation processes focused on hydrogen production.

Finally, when N₂ gas used as nitrogen source (R14), negligible H₂ production was observed (Table 2). Moreover, cell growth rate (3.3 ± 2.1 mgVSS/Lh) and substrate consumption rate were significantly lower for the N₂-purged reactors than in any other condition using malic acid (R1–R4 and R9–R11) (Table 2). This could be attributed to the N₂ passing from the gas to the liquid phase, which could be characterized as the rate-limiting step of the process. In addition, N₂ fixation competes with hydrogen production for the reduced cofactors generated during oxidation of organic substrates into biomass. Hydrogen production under nitrogen fixation conditions is an inefficient process as 75% of electrons go to ammonia generation purposes. However, in the absence of N₂, nitrogenase exclusively reduces protons towards maximal H₂ production [14]. These findings are in accordance with other studies, reporting that the amount of H₂ produced from propionate and butyrate, decreased under N₂ gas phase growth of *R. sphaeroides* [19].

3.3. Effect of Carbon Sources on H₂ and CO₂ Production

In order to compare the effect of carbon source used, experimental runs (R5–R8, Table 2), were conducted using similar concentrations of NH₄-N (75–600 mgNH₄-N/L, 5.4–42.9 mM ammonium), but acetic acid as carbon source rather than malic acid. Results showed no H₂ or CO₂ production at any ammonium concentration used; however, PPB growth rates were comparable to those achieved by malic acid (Table 2). In addition, lower organic substrate assimilation rates were observed when acetic acid was used as carbon source. Acetic acid uptake also caused a rise in pH values more than 9. This pH increase has been related to the metabolic pathway of poly-β-hydroxybutyrate (PHB) formation rather than H₂ production [20]. Accumulation of PHB can affect the acid-base equilibrium and rise the pH value in the cultivation medium. Therefore, it may be assumed that the excess of electrons was accumulated as PHB instead of released as H₂. The PHB accumulation of PHA as an electron sink using acetate as carbon source has been previously demonstrated in *R. sphaeroides* cultures [21,22].

Furthermore, a set of experiments was carried out with Na-glutamate as N source but including two additional carbon sources, acetic acid and butyric acid, instead of malic acid. The concentrations used were 300 mgN/L as Na-glutamate and 9.5 mM (ca. 0.5 gC/L) of butyric acid (R12) and 25 mM (ca. 0.60 gC/L) of acetic acid (R13), respectively. Figure 7a,b represents the organic substrates' degradation and PPB growth of two experimental trials (1 and 2), while Figure 7c,d shows the H₂ and CO₂ production by PPB. Table 2 summarizes the photo-H₂ production, H₂ yield, cell growth rate and CO₂ emissions of the mixed PPB culture using the two carbon sources and glutamate as nitrogen source. The total amount of H₂ produced after one week of cultivation was 145.2 ± 31.6 and 94.6 ± 7.5 mLH₂/L for the butyric (R12) and acetic (R13) experiments, respectively, which were anyway much lower than the achieved in the malic experiment (R11, 370.0 ± 27.4 mLH₂/L, Table 2). These findings are related to the different entrance of the substrates in the central metabolism of PPB, since malate enters directly into the TCA cycle, and therefore reductants go to succinate/fumarate that can drive direct energy production [10]. Accordingly, the H₂ production rate achieved was 2.3 ± 0.2 mLH₂/Lh, 0.86 ± 0.19 mLH₂/Lh and 0.56 ± 0.04 mLH₂/Lh for malic, butyric and acetic acids, respectively (Table 2).

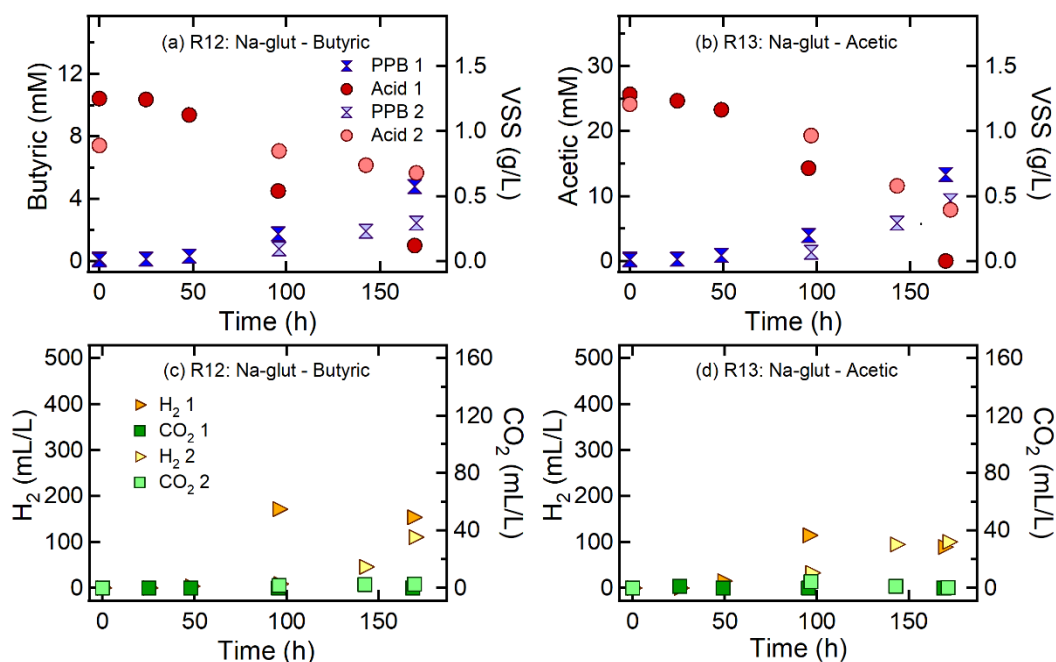


Figure 7. Acids' assimilation, PPB growth and gases' production in media supplemented with (a,c) butyric acid and Na-glutamate for R12 and (b,d) acetic acid and Na-glutamate for R13.

Apart from the H₂ production rate achieved, another criterion to evaluate the hydrogen production performance of an organic substrate is the substrate conversion efficiency. This means the amount of the substrate that has been utilized for hydrogen production instead of cell growth. The conversion efficiency can be evaluated by Equation (6).

$$\% \text{ Conversion efficiency} = 100 \cdot \frac{\text{Actual H}_2 \text{ moles produced}}{\text{Theoretical H}_2 \text{ moles}} \quad (6)$$

The theoretical amount of hydrogen was evaluated assuming that all the acid's substrate was converted to H₂ and CO₂ [46]. Results showed that the conversion efficiency achieved by the mixed PPB culture was in the order of butyric (9.3%) > malic (6.5%) > acetic acid (4.4%). However, the conversion efficiencies observed in this study, were lower than those reported for pure PPB cultures [10]. Specifically, other studies, working with PPB species, such as *R. sphaeroides* or *R. capsulatus*, observed a 22–56% substrate conversion efficiency with malate as carbon source [47–49]. Moreover, researchers working with butyrate or acetate as carbon sources, reported substrates conversions in the range of 40–75% by *R. monas* or *R. sphaeroides* [50,51].

The conversion efficiency of each substrate, was also verified by evaluating the electron partitioning during growth and H₂ production process, following the procedure outlined by Yilmaz et al. [16]. Therefore, the concentrations of carbon and nitrogen substrates were converted into COD to quantify electron availability and partitioning in different electron sinks. The reducing power was equal to the sum of COD in the carbon source and in glutamate, that were consumed at the end of each experiment. The PPB growth was converted into COD, considering that 1 mg PPB expressed as VSS equals to 1.78 mg COD [13]. The theoretical value of COD for H₂ production was calculated as 16 mgCOD / mmol of H₂. The fate of substrate electrons in PPB cultures cultivated with different carbon sources are shown in Figure 8. All the COD values have been normalized dividing by the total COD consumed during each test (R11, R12, R13). The data indicated that, in malate-fed culture, the fraction of substrate electrons converted to cell synthesis was 64% (f_{cells}), while the fraction of substrate electron used for H₂ formation was 5.8% (f_{H_2}). In addition, when butyric and acetic acids were used as carbon sources, 50% and 48% of electrons were partitioned into the cell growth and 6.1% and 2.1% of electrons were partitioned into H₂ production, respectively. This is in accordance with the higher yield (Y_{H_2}) observed

for butyric (0.4 LH₂/g acid) as compare to acetic acid (0.16 LH₂/g acid) (Table 2). Notably, it has been reported that the fraction of substrate electrons used for the cell growth of *Rhodobacter sphaeroides* was higher using butyrate or acetate (85%) than malate (48%) as organic substrate [43]. It was observed, that based on the theoretical calculation $f_{other} = 100 - f_{H_2} - f_{cells}$, more than 30% of the reducing power in all cases, tends to be partitioned into other electron sinks. If the energy used for cell maintenance has a minor portion, f_{other} could be correlated with soluble microbial products (SMPs), which are accumulated to the culture media due to cell lysis or are excreted for metabolic purposes [43]. The SMPs accumulated in this study in each case (Figure 8, R11, R12 and R13), were calculated by subtracting the COD of the remaining carbon and nitrogen sources from the measured soluble COD in the media [16]. It was observed, that the calculated SMPs (26% for malic, 54% for butyric and 55% for acetic) were similar to the theoretical calculated fraction f_{other} (30% for malic, 45% for butyric and 50% for acetic). These results are in agreement with the findings reported by Yilmaz et al. [16], who observed that SMP was a major electron sink (>30% of the substrate electrons especially in resting cells), taking a big fraction of reducing power away from H₂ production, in *R. sphaeroides* cultures. SMP formation during photoheterotrophic growth, may be associated with the formation of metabolic byproducts, such as formate, as well as high-molecular weight extracellular polymeric substances (EPS).

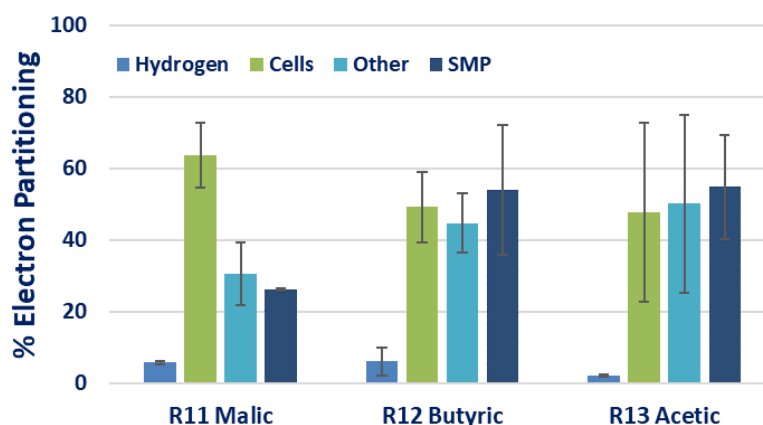


Figure 8. Electron partitioning during PPB growth using different organic substrates. Error bars present the represent the standard deviation of data.

An important electron sink, that is correlated with f_{cells} , is the CO₂ fixation, as an electron accepting process. It is well known, that under butyrate-fed conditions, the role of CO₂ fixation during PPB growth is to accept electrons, generated during the conversion of the reduced carbon source to PPB biomass, in order to maintain the redox balance [11]. As a result, negligible CO₂ emission was occurred during the R12 experiment (Table 2). Negligible CO₂ was observed in the case of acetic acid (Table 2), which is slightly more oxidized than the PPB biomass. McKinlay and Harwood [11] demonstrate that CO₂ fixation is required for *R. palustris* photoheterotrophic growth on acetate, as about two times more reduced redox cofactors are produced than is required for biosynthesis during acetate uptake. Therefore, CO₂ fixation is an obligatory electron-accepting process for the recycle of the excess of reduced cofactors.

In summary, the PPB mixed culture was able to produce significant amount of H₂ using malic acid as carbon source, while the use of glutamate decreases CO₂ emissions. The negative correlation between glutamate's concentration and CO₂ gas production, suggests that wastewater with high organic nitrogen content may be a preferable feedstock to produce H₂ using PPB mixed cultures. It has been reported, that wastewaters produced from industrial processes, have less microbial (e.g., pathogens), metal, and organic contaminants content than domestic wastewater [33]. Therefore, animal processing wastewaters (e.g., poultry processing wastewater), with high concentration of nutrients and organic carbon, are potential good candidates to drive H₂ production by PPB with low C footprint.

Table 2. H₂ and CO₂ production by PPB under different nitrogen and carbon sources.

RUN Number	Carbon Source	Nitrogen Source	Nitrogen (mgN/L)	COD-Substrate to N Ratio ^a COD:N	Measured COD to N Ratio ^b COD:N	R _{PPB} ^c (mgVSS/Lh)	R _{acid} ^d (mM acid/h)	H ₂ ^e (mLH ₂ /L)	H ₂ _{rate} ^f (mLH ₂ /Lh)	Y _{H₂} ^g (LH ₂ /g_Acid)	CO ₂ ^h (mLCO ₂ /L)
R1	Malic acid	NH ₄ Cl	75	100:3.8	100:3	3.7 ± 0.8	0.32 ± 0.11	381.6 ± 13.2	2.5 ± 0.8	0.11 ± 0.01	51.2 ± 1.6
R2			150	100:7.5	100:6.8	3.7 ± 1.7	0.28 ± 0.10	1.4 ± 2.1	0 ± 0	0 ± 0	5.6 ± 3.0
R3			300	100:15	100:12.1	4.2 ± 2.3	0.26 ± 0.11	1.8 ± 2.9	0 ± 0	0 ± 0	11.0 ± 1.7
R4			600	100:30	100:33.8	1.69	0.31	0	0	0	15.1
R5	Acetic acid	NH ₄ Cl	75	100:3.8	100:2.9	3.62	0.11	0	0.01	0.002	0
R6			150	100:7.5	100:8.6	2.93	0.07	2.4	0.02	0.004	0
R7			300	100:15	100:15.6	3.95	0.12	2.9	0.02	0.002	0
R8			600	100:30	100:44	4.30	0.09	2.8	0	0	0.2
R9	Malic acid	Na-glutamate	75	100:3.8	100:2.3	3.8 ± 0.5	0.31 ± 0.08	264.3 ± 96.4	1.7 ± 0.8	0.08 ± 0.03	66.4 ± 6.1
R10			150	100:7.5	100:4.6	4.6 ± 2.9	0.23 ± 0.12	305.9 ± 64.2	2.1 ± 0.9	0.12 ± 0.05	38.2 ± 21.4
R11			300	100:15	100:5.5	6.9 ± 2.4	0.30 ± 0.05	370.0 ± 27.4	2.3 ± 0.2	0.11 ± 0.01	13.4 ± 13.6
R12	Butyric acid	Na-glutamate	300	100:15	100:6.9	2.7 ± 0.9	0.04 ± 0.03	145.2 ± 31.6	0.86 ± 0.19	0.40 ± 0.28	1.1 ± 1.3
R13	Acetic acid	Na-glutamate	300	100:15	100:6.7	3.3 ± 0.9	0.10 ± 0.08	94.6 ± 7.5	0.56 ± 0.04	0.16 ± 0.15	0.10 ± 0.12
R14	Malic acid	N ₂ gas	650	100:33	100:36	3.3 ± 2.1	0.01 ± 0	1.7 ± 0	0 ± 0	0 ± 0	1.6 ± 1.9

^a COD-substrate to N ratio, considering only the COD of organic substrate and the N of the nitrogen substrate; ^b Measured COD to N ratio, considering also the COD content of glutamate;

^c PPB growth rate; ^d organic substrate assimilation rate; ^e H₂ production; ^f H₂ production rate; ^g H₂ yield, ^h CO₂ production.

4. Conclusions

In this study, a mixed PPB culture was used to assess the effects of organic carbon and nitrogen substrates' on H₂ production as well as on CO₂ emissions by the PPB culture. Results suggested that malic acid was more favorable organic source than butyric and acetic acids for H₂ formation, achieving higher production rate. Moreover, NH₄-N and Na-glutamate were found to produce comparable amounts of H₂ when they used in combination with malic acid, in COD:N ratios of 100:3 and 100:5.5, respectively. However, the use of high glutamate's concentration favors CO₂ mitigation emissions. The experimental findings presented herein are useful to better plan wastewater treatment strategies by PPB mixed cultures for H₂ production with low CO₂ emissions.

Author Contributions: This work was carried out in collaboration between all authors. I.A.V. designed the study, performed the experimental investigation, the data curation, the statistical analysis and wrote the first draft of the manuscript; F.M. and J.A.M. performed the supervision and the writing—review; R.M. and D.P. performed the writing—review and the editing; D.P. performed the supervision, designed the study and performed the data analysis. All authors have read and agreed to the published version of the manuscript.

Funding: “This research was funded by the INTERNATIONAL EXCELLENCE CAMPUS “SMART ENERGY” PROGRAM (CEISEP–Post-doctoral Fellowship of I.A.V.), “Comunidad de Madrid” and European Structural Funds by the REMTAVARES-CM project (S2018/EMT-4341) and Spanish Ministry of Economy by the FOTOBIOELECTRO project (CTM2017-91186-EXP).

Conflicts of Interest: The authors declare no conflict of interest.

References

1. Batstone, D.J.; Hülsen, T.; Mehta, C.M.; Keller, J. Platforms for energy and nutrient recovery from domestic wastewater: A review. *Chemosphere* **2015**, *140*, 2–11. [[CrossRef](#)]
2. Garcia, D.J.; You, F. The water-energy-food nexus and process systems engineering: A new focus. *Comput. Chem. Eng.* **2016**, *91*, 49–67. [[CrossRef](#)]
3. Hülsen, T.; Batstone, D.J.; Keller, J. Phototrophic bacteria for nutrient recovery from domestic wastewater. *Water Res.* **2014**, *50*, 18–26. [[CrossRef](#)]
4. Zimmo, O.; van der Steen, P.; Gijzen, H. Nitrogen mass balance across pilot-scale algae and duckweed-based wastewater stabilisation ponds. *Water Res.* **2004**, *38*, 913–920. [[CrossRef](#)]
5. Lavrinovičs, A.; Juhna, T. Review on Challenges and Limitations for Algae-Based Wastewater Treatment. *Constr. Sci.* **2017**, *20*, 17–25. [[CrossRef](#)]
6. Hülsen, T.; Barry, E.M.; Lu, Y.; Puyol, D.; Batstone, D.J. Low temperature treatment of domestic wastewater by purple phototrophic bacteria: Performance, activity, and community. *Water Res.* **2016**, *100*, 537–545. [[CrossRef](#)]
7. Zhang, D.; Yang, H.; Huang, Z.; Liu, S.-J. *Rhodocista pekingensis* sp. nov., a cyst-forming phototrophic bacterium from a municipal wastewater treatment plant. *Int. J. Syst. Evol. Microbiol.* **2003**, *53*, 1111–1114. [[CrossRef](#)]
8. Basak, N.; Das, D. The Prospect of Purple Non-Sulfur (PNS) Photosynthetic Bacteria for Hydrogen Production: The Present State of the Art. *World J. Microbiol. Biotechnol.* **2006**, *23*, 31–42. [[CrossRef](#)]
9. Kim, M.K.; Choi, K.-M.; Yin, C.-R.; Lee, K.-Y.; Im, W.-T.; Lim, J.H.; Lee, S.-T. Odorous swine wastewater treatment by purple non-sulfur bacteria, *Rhodospseudomonas palustris*, isolated from eutrophicated ponds. *Biotechnol. Lett.* **2004**, *26*, 819–822. [[CrossRef](#)]
10. Koku, H. Aspects of the metabolism of hydrogen production by *Rhodobacter sphaeroides*. *Int. J. Hydrog. Energy* **2002**, *27*, 1315–1329. [[CrossRef](#)]
11. McKinlay, J.B.; Harwood, C.S. Carbon dioxide fixation as a central redox cofactor recycling mechanism in bacteria. *Proc. Natl. Acad. Sci. USA* **2010**, *107*, 11669–11675. [[CrossRef](#)]
12. Mckinlay, J.B.; Harwood, C.S. Calvin Cycle Flux, Pathway Constraints, and Substrate Oxidation State Bacteria. *mBio* **2011**, *2*, 1–9. [[CrossRef](#)]
13. Puyol, D.; Barry, E.; Hülsen, T.; Batstone, D.J. A mechanistic model for anaerobic phototrophs in domestic wastewater applications: Photo-anaerobic model (PAnM). *Water Res.* **2017**, *116*, 241–253. [[CrossRef](#)]

14. Rey, F.E.; Heiniger, E.; Harwood, C.S. Redirection of Metabolism for Biological Hydrogen Production. *Appl. Environ. Microbiol.* **2007**, *73*, 1665–1671. [[CrossRef](#)]
15. Vasiliadou, I.; Berná, A.; Manchon, C.; Melero, J.A.; Martinez, F.; Esteve-Nuñez, A.; Puyol, D. Biological and Bioelectrochemical Systems for Hydrogen Production and Carbon Fixation Using Purple Phototrophic Bacteria. *Front. Energy Res.* **2018**, *6*, 107. [[CrossRef](#)]
16. Yilmaz, L.S.; Kontur, W.S.; Sanders, A.P.; Sohmen, U.; Donohue, T.J.; Noguera, D.R. Electron Partitioning During Light- and Nutrient-Powered Hydrogen Production by *Rhodobacter sphaeroides*. *BioEnergy Res.* **2010**, *3*, 55–66. [[CrossRef](#)]
17. Tao, Y. Characteristics of a new photosynthetic bacterial strain for hydrogen production and its application in wastewater treatment. *Int. J. Hydrog. Energy* **2008**, *33*, 963–973. [[CrossRef](#)]
18. Sasikala, C.H.; Ramana, C.H.V.; Rao, P.R. Regulation of simultaneous hydrogen photoproduction during growth by pH and glutamate in *Rhodobacter sphaeroides* O.U. 001. *Int. J. Hydrog. Energy* **1995**, *20*, 123–126. [[CrossRef](#)]
19. Ventura, R.L.G.; Ventura, J.R.S.; Oh, Y.S. Photoheterotrophic hydrogen production of *rhodobacter sphaeroides* KCTC 1434 under alternating air and N₂ headspace gas. *Philipp. J. Sci.* **2019**, *148*, 63–72.
20. Fang, H.; Liu, H.; Zhang, T. Phototrophic hydrogen production from acetate and butyrate in wastewater. *Int. J. Hydrog. Energy* **2005**, *30*, 785–793. [[CrossRef](#)]
21. Lee, H.-S.; Vermaas, W.F.; Rittmann, B.E. Biological hydrogen production: Prospects and challenges. *Trends Biotechnol.* **2010**, *28*, 262–271. [[CrossRef](#)]
22. Craven, J.; Sultan, M.A.; Sarma, R.; Wilson, S.; Meeks, N.; Kim, D.Y.; Hastings, J.T.; Bhattacharyya, D. *Rhodospseudomonas palustris*-based conversion of organic acids to hydrogen using plasmonic nanoparticles and near-infrared light. *RSC Adv.* **2019**, *9*, 41218–41227. [[CrossRef](#)]
23. Wu, T.Y.; Hay, J.X.W.; Kong, L.B.; Juan, J.C.; Jahim, J.M. Recent advances in reuse of waste material as substrate to produce biohydrogen by purple non-sulfur (PNS) bacteria. *Renew. Sustain. Energy Rev.* **2012**, *16*, 3117–3122. [[CrossRef](#)]
24. Chiemchaisri, C.; Jaitrong, L.; Honda, R.; Fukushi, K.; Yamamoto, K. Photosynthetic bacteria pond system with infra-red transmitting filter for the treatment and recovery of organic carbon from industrial wastewater. *Water Sci. Technol.* **2007**, *56*, 109–116. [[CrossRef](#)]
25. Lee, M.G.; Kobayashi, M. Deodorization of swine sewage by addition of a phototrophic bacterium, *Rhodospseudomonas capsulata*. *Soil Sci. Plant Nutr.* **1992**, *38*, 767–770. [[CrossRef](#)]
26. Lo, Y.-C.; Chen, C.-Y.; Lee, C.-M.; Chang, J.-S. Photo fermentative hydrogen production using dominant components (acetate, lactate, and butyrate) in dark fermentation effluents. *Int. J. Hydrog. Energy* **2011**, *36*, 14059–14068. [[CrossRef](#)]
27. Tawfik, A.; El-Bery, H.; Singh, G.; Bux, F. Use of mixed culture bacteria for photofermentive hydrogen of dark fermentation effluent. *Bioresour. Technol.* **2014**, *168*, 119–126. [[CrossRef](#)]
28. Kantachote, D.; Torpee, S.; Umsakul, K. The potential use of anoxygenic phototrophic bacteria for treating latex rubber sheet wastewater. *Electron. J. Biotechnol.* **2005**, *8*, 314–323. [[CrossRef](#)]
29. Zhu, H.; Suzuki, T.; Tsygankov, A.; Asada, Y.; Miyake, J. Hydrogen production from tofu wastewater by *Rhodobacter sphaeroides* immobilized in agar gels. *Int. J. Hydrog. Energy* **1999**, *24*, 305–310. [[CrossRef](#)]
30. Yetis, M. Photoproduction of hydrogen from sugar refinery wastewater by *Rhodobacter sphaeroides* O.U. 001. *Int. J. Hydrog. Energy* **2000**, *25*, 1035–1041. [[CrossRef](#)]
31. Serna, R.L.; Garcia, D.; Bolado, S.; Jiménez, J.J.; Lai, F.Y.; Golovko, O.; Gago-Ferrero, P.; Ahrens, L.; Wiberg, K.; Munoz, R. Photobioreactors based on microalgae-bacteria and purple phototrophic bacteria consortia: A promising technology to reduce the load of veterinary drugs from piggery wastewater. *Sci. Total. Environ.* **2019**, *692*, 259–266. [[CrossRef](#)]
32. Hülsen, T.; Hsieh, K.; Lu, Y.; Tait, S.; Batstone, D.J. Simultaneous treatment and single cell protein production from agri-industrial wastewaters using purple phototrophic bacteria or microalgae—A comparison. *Biores. Technol.* **2018**, *254*, 214–223. [[CrossRef](#)]
33. Hülsen, T.; Hsieh, K.; Tait, S.; Barry, E.M.; Puyol, D.; Batstone, D.J. White and infrared light continuous photobioreactors for resource recovery from poultry processing wastewater—A comparison. *Water Res.* **2018**, *144*, 665–676. [[CrossRef](#)]
34. Hülsen, T.; Hsieh, K.; Batstone, D.J. Saline wastewater treatment with purple phototrophic bacteria. *Water Res.* **2019**, *160*, 259–267. [[CrossRef](#)]

35. Dalaei, P.; Bahreini, G.; Nakhla, G.; Santoro, D.; Batstone, D.; Hülsen, T. Municipal wastewater treatment by purple phototrophic bacteria at low infrared irradiances using a photo-anaerobic membrane bioreactor. *Water Res.* **2020**, *173*, 115535. [[CrossRef](#)]
36. Hu, J.; Yang, H.; Wang, X.; Cao, W.; Guo, L. Strong pH dependence of hydrogen production from glucose by *Rhodobacter sphaeroides*. *Int. J. Hydrog. Energy* **2020**, *45*, 9451–9458. [[CrossRef](#)]
37. Ormerod, J.G.; Ormerod, K.S.; Gest, H. Light-Dependent Utilization of Organic Compounds Photoproduction of Molecular Hydrogen by Photosynthetic Bacteria; Relationships with Nitrogen Metabolism' of organic com- grown with N, or certain amino acids pro- duce large quantities of molecular hydr. *Arch. Biochem. Biophys.* **1961**, *94*, 449–463. [[PubMed](#)]
38. Clemens, P.; Walter, C. *Microalgal Biotechnology: Potential and Production*; Walter de Gruyter: Berlin, Germany, 2012; ISBN 978-3-11-022501-3.
39. APHA. *Standard Methods for the Examination of Water and Wastewater Standard Methods for the Examination of Water and Wastewater*, 17th ed.; American Public Health Association: Washington, DC, USA, 1989.
40. Heras, I.D.L.; Molina, R.; Segura, Y.; Hülsen, T.; Molina, M.; Gonzalez-Benitez, N.; Melero, J.; de la Rubia, M.; Martínez, F.; Puyol, D. Contamination of N-poor wastewater with emerging pollutants does not affect the performance of purple phototrophic bacteria and the subsequent resource recovery potential. *J. Hazard. Mater.* **2020**, *385*, 121617. [[CrossRef](#)]
41. Melnicki, M.; Bianchi, L.; de Philippis, R.; Melis, A. Hydrogen production during stationary phase in purple photosynthetic bacteria. *Int. J. Hydrog. Energy* **2008**, *33*, 6525–6534. [[CrossRef](#)]
42. Niedzwiedzki, D.M.; Dilbeck, P.L.; Tang, Q.; Martin, E.C.; Bocian, D.F.; Hunter, C.N.; Holten, D. New insights into the photochemistry of carotenoid spheroidenone in light-harvesting complex 2 from the purple bacterium *Rhodobacter sphaeroides*. *Photosynth. Res.* **2016**, *131*, 291–304. [[CrossRef](#)]
43. Kim, M.-S.; Kim, D.-H.; Cha, J. Culture conditions affecting H₂ production by phototrophic bacterium *Rhodobacter sphaeroides* KD131. *Int. J. Hydrog. Energy* **2012**, *37*, 14055–14061. [[CrossRef](#)]
44. Tichi, M.A.; Tabita, F.R. Maintenance and control of redox poise in *Rhodobacter capsulatus* strains deficient in the Calvin-Benson-Bassham pathway. *Arch. Microbiol.* **2000**, *174*, 322–333. [[CrossRef](#)]
45. Wang, X.; Falcone, D.L.; Tabita, F.R. Reductive pentose phosphate-independent CO₂ fixation in *Rhodobacter sphaeroides* and evidence that ribulose biphosphate carboxylase/oxygenase activity serves to maintain the redox balance of the cell. *J. Bacteriol.* **1993**, *175*, 3372–3379. [[CrossRef](#)] [[PubMed](#)]
46. Sasikala, K.; Ramana, C.; Rao, P.R.; Kovács, K. Anoxygenic Phototrophic Bacteria: Physiology and Advances in Hydrogen Production Technology. *Nat. Eng. Resist. Plant Vir. Part II* **1993**, *38*, 211–295. [[CrossRef](#)]
47. Hillmer, P.; Gest, H. H₂ metabolism in the photosynthetic bacterium *Rhodospseudomonas capsulata*: Production and utilization of H₂ by resting cells. *J. Bacteriol.* **1977**, *129*, 732–739. [[CrossRef](#)] [[PubMed](#)]
48. Eroglu, N.; Aslan, K.; Gündüz, U.; Yücel, M.; Turker, L. Substrate consumption rates for hydrogen production by *Rhodobacter sphaeroides* in a column photobioreactor. *Biotransform. Microb. Degrada. Health-Risk Compd.* **1999**, *35*, 103–113. [[CrossRef](#)]
49. Eroglu, I. Hydrogen production by *Rhodobacter sphaeroides* O.U.001 in a flat plate solar bioreactor. *Int. J. Hydrog. Energy* **2008**, *33*, 531–541. [[CrossRef](#)]
50. Mao, X.-Y.; Miyake, J.; Kawamura, S. Screening photosynthesis bacteria for hydrogen production from organic acids. *J. Ferment. Technol.* **1986**, *64*, 245–249. [[CrossRef](#)]
51. Barbosa, M.J.; Rocha, J.; Tramper, J.; Wijffels, R.H. Acetate as a carbon source for hydrogen production by photosynthetic bacteria. *J. Biotechnol.* **2001**, *85*, 25–33. [[CrossRef](#)]

